ECOGRAPHY

Software note

'LandsatTS': an R package to facilitate retrieval, cleaning, cross-calibration, and phenological modeling of Landsat time series data

Logan T. Berner[1], **Jakob J. Assmann**[2,3], **Signe Normand**[2] **and Scott J. Goetz**[1]

[1]School of Informatics, Computing, and Cyber Systems, Northern Arizona University, Flagstaff, USA
[2]Department of Biology, Ecoinformatics and Biodiversity, Aarhus University, Aarhus, Denmark
[3]Department of Evolutionary Biology and Environmental Studies, University of Zurich, Zurich, Switzerland

Correspondence: Logan T. Berner (logan.berner@nau.edu)

Ecography
2023: e06768
doi: 10.1111/ecog.06768
Subject Editor:
Michael Krabbe Borregaard
Editor-in-Chief: Miguel Araújo
Accepted 24 April 2023

The Landsat satellites provide decades of near-global surface reflectance measurements that are increasingly used to assess interannual changes in terrestrial ecosystem function. These assessments often rely on spectral indices related to vegetation greenness and productivity (e.g. Normalized Difference Vegetation Index, NDVI). Nevertheless, multiple factors impede multi-decadal assessments of spectral indices using Landsat satellite data, including ease of data access and cleaning, as well as lingering issues with cross-sensor calibration and challenges with irregular timing of cloud-free acquisitions. To help address these problems, we developed the 'LandsatTS' package for R. This software package facilitates sample-based time series analysis of surface reflectance and spectral indices derived from Landsat sensors. The package includes functions that enable the extraction of the full Landsat 5, 7, and 8 records from Collection 2 for point sample locations or small study regions using Google Earth Engine accessed directly from R. Moreover, the package includes functions for 1) rigorous data cleaning, 2) cross-sensor calibration, 3) phenological modeling, and 4) time series analysis. For an example application, we show how 'LandsatTS' can be used to assess changes in annual maximum vegetation greenness from 2000 to 2022 across the Noatak National Preserve in northern Alaska, USA. Overall, this software provides a suite of functions to enable broader use of Landsat satellite data for assessing and monitoring terrestrial ecosystem function during recent decades across local to global geographic extents.

Keywords: cross-sensor calibration, Google Earth Engine, greening and browning, Landsat, NDVI, spectral index

Background

Satellite remote sensing is crucial for assessing and monitoring how Earth's terrestrial ecosystems have changed during recent decades (National Academies of Sciences 2018). The Landsat satellites are particularly valuable in this regard because they are

the longest continuously running satellite program and were designed for terrestrial ecosystem monitoring at moderate spatial resolution (Wulder et al. 2019). The first Landsat satellite (Landsat 1) was launched in 1972 as a partnership between NASA and the US Geological Survey (USGS) and since that time a series of additional satellites have been launched, with the most recent being Landsat 9 in 2021. The Landsat satellites carry multispectral sensors that provide surface reflectance measurements used for a wide range scientific and land management applications (Wulder et al. 2019). These include global monitoring of changes in forest canopy cover (Hansen et al. 2013, Sexton et al. 2013), land cover and use (Potapov et al. 2022), and surface water extent (Pekel et al. 2016), as well as regional- to biome-scale assessments of how disturbance, land-use, and climate change are impacting terrestrial ecosystems (Wulder et al. 2004, Powell et al. 2010, Ju and Masek 2016, Wang and Friedl 2019). Hence, the Landsat program has become a cornerstone of Earth surface monitoring. Yet there are challenges that hinder use of these data by ecologists, land managers, and other non-remote sensing specialists.

Here we present the 'LandsatTS' (i.e., Landsat Time Series) software package for R (www.r-project.org) that enables users to extract, process, and analyze time series of Landsat surface reflectance measurements for sample locations anywhere on Earth. 'LandsatTS' enables extraction of Landsat 5, 7, and 8 surface reflectance measurements from the full Landsat Collection 2 dataset on Google Earth Engine (GEE; Gorelick et al. 2017). Furthermore, 'LandsatTS' includes functions that facilitate 1) data cleaning, 2) cross-sensor calibration, 3) phenological modeling, and 4) time series analysis of vegetation greenness (Fig. 1, Table 1). This software grew out of research projects focused on vegetation dynamics across northern high-latitude ecosystems (Berner et al. 2020, Berner and Goetz 2022) and is implemented within the free, open-source, and widely used R statistical computing environment (R Core Team 2021).

It has become easier to access and process Landsat data since the archive was made publicly available in 2008 (Wulder et al. 2012) and a copy of the archive subsequently hosted on GEE (Gorelick et al. 2017). The GEE cloud-computing platform enables users to access and process Landsat data using JavaScript and Python application program interfaces (APIs), as well as with R through the 'rgee' package (www.r-project.org, Aybar et al. 2020). R is very popular among ecologists (Lai et al. 2019), yet other existing R packages (www.r-project.org) only provide tools for processing individual Landsat scenes. For instance, 'landsat' includes functions for radiometric and topographic correction of Landsat scenes (Goslee 2011), while 'landsat8' includes functions for computing top of atmosphere reflectance, radiance, and/or brightness temperature on Landsat scenes (dos Santos 2017). Thus, the 'rgee' package makes it easier for ecologists to use the GEE platform and work with Landsat data. Nevertheless, it remains non-trivial to not only extract Landsat time series data using 'rgee', but also to thoroughly clean the extracted data to ensure that only high-quality measurements are used in analyses. 'LandsatTS' therefore provides new tools for sample-based extraction of full Landsat data records using 'rgee' to access the GEE. Furthermore, 'LandsatTS' includes tools to rigorously clean Landsat data using both pixel-level CFmask flags (e.g. cloud, water; Zhu et al. 2015) and scene-level criteria (e.g. cloud cover, solar zenith angle). Consequently, 'LandsatTS' helps further broaden the community of researchers who can utilize Landsat data for robust spatiotemporal analyses of terrestrial ecosystem dynamics.

Landsat time series analyses that use measurements from multiple sensors are hindered by systematic biases in spectral bands and indices among the Landsat 5 Thematic Mapper (TM), Landsat 7 Enhanced Thematic Mapper Plus (ETM+), and Landsat 8 Operational Land Imager (OLI) sensors (Ju and Masek 2016, Roy et al. 2016, Berner et al. 2020, Berner and Goetz 2022). If unaccounted for, these biases can introduce pronounced artificial trends into combined time series, such as spurious increases over time in spectral indices of vegetation greenness including the widely used Normalized Difference Vegetation Index (NDVI) (Sulla-Menashe et al. 2017). Prior approaches for cross-sensor calibration focused on linear corrections for individual spectral bands and select spectral indices (e.g. NDVI) using regional data (e.g. continental USA) from Landsat Collection 1 (Ju and Masek 2016, Roy et al. 2016). While valuable, these published cross-sensor calibration models do not account for potential non-linearities, may not be suitable for other regions, and may not be appropriate for the newer Landsat Collection 2 dataset. Therefore, 'LandsatTS' includes functions to cross-calibrate spectral bands and indices among Landsat 5, 7, and 8 using either random forest machine learning or polynomial regression models. These models can be fit using the user's dataset. However, if the user's dataset is too small to fit these models, then, if appropriate, the user can choose to fit models using pre-processed and staged Landsat data that were sampled from across the Arctic tundra and boreal forest biomes. See Supporting information for polynomial regression model coefficients and evaluation metrics for this domain for each spectral band and select indices (e.g. NDVI, EVI2, NBR). Flexible implementation of cross-sensor calibration in the 'LandsatTS' workflow enables the user to generate high-quality time series that are free from sensor-specific biases that can otherwise induce spurious trends.

Vegetation phenology controls ecosystem processes (e.g. photosynthesis) and is often assessed using spectral indices (e.g. NDVI) derived from satellite measurements (Helman 2018, Zeng et al. 2020). Nevertheless, efforts to assess vegetation phenology using the Landsat satellites are complicated by multiple factors that include 1) irregular timing of clear-sky acquisitions within a growing season and 2) changes in the annual number of clear-sky acquisitions across years as new satellites were launched. These challenges are especially acute in regions with short, cloudy growing seasons such as the Arctic, where the median number of clear-sky growing season measurements increased from 2 per year in 1995 to 7 per year in 2015 (Berner et al. 2020). Annual maximum

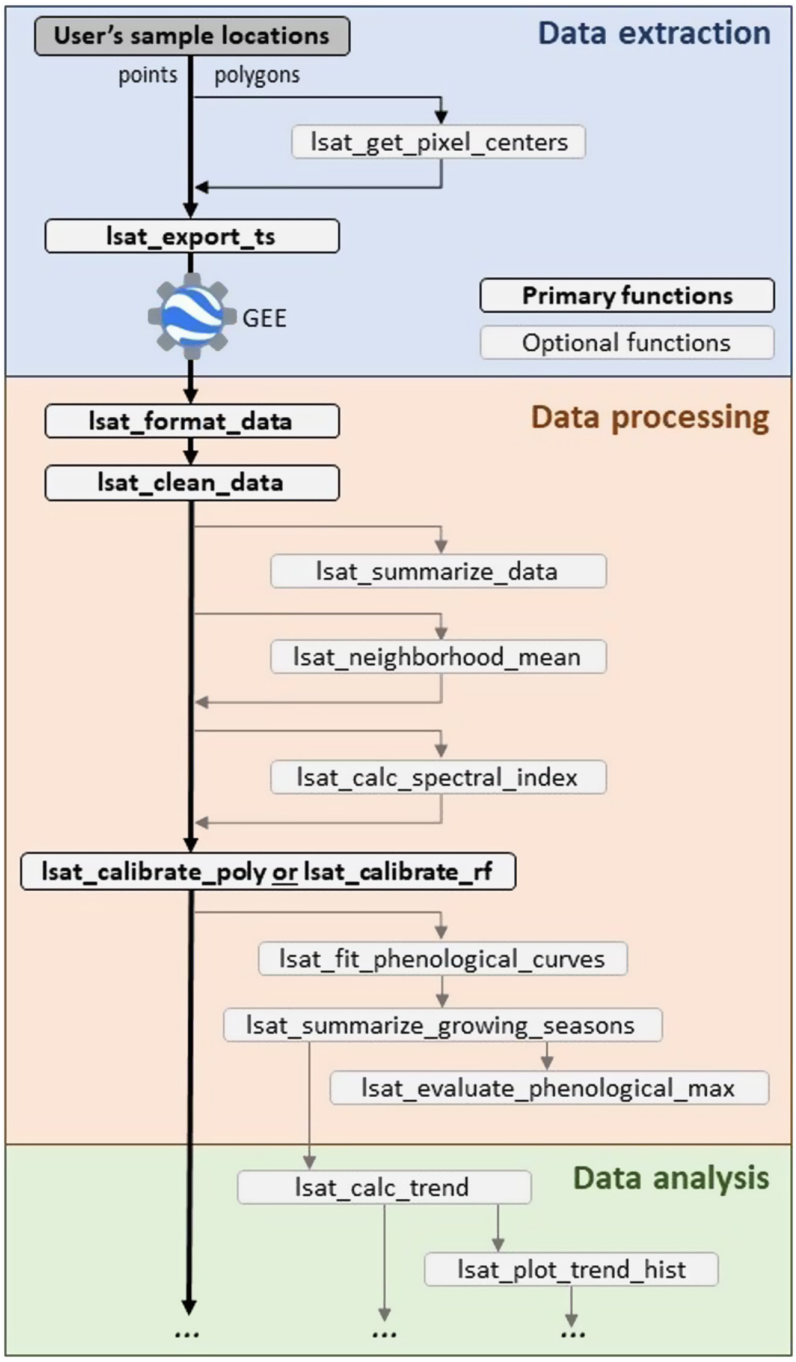

Figure 1. Schematic illustrating functions and typical workflow of the 'LandsatTS' package. Each function is briefly described in Table 1, with further details provided in the Supporting information and package documentation. 'LandsatTS' has primary been used for assessments of interannual variability and trends in vegetation greenness. However, 'LandsatTS' facilitates other Landsat time series analyses by providing tools for general data extraction and processing. GEE, Google Earth Engine.

vegetation greenness is an important metric of vegetation phenology related to productivity (Berner et al. 2020, Zeng et al. 2020, Boyd et al. 2021), yet this metric is sensitive to the timing and number of measurements made in a growing season. Consequently, simple calculations of this metric tend to be artificially low early in the Landsat record but less so during later years when more measurements are available, which can introduce a spurious positive trend into a time series (Berner et al. 2020). To address this issue, 'LandsatTS' includes tools to estimate annual maximum vegetation greenness based on site-specific phenological modeling that iteratively fits cubic splines to vegetation greenness time series. Users interested in other aspects of vegetation phenology (e.g. timing of spring onset or fall senescence) could extract and

Table 1. Function names and descriptions. These are listed in the order typically used. A more detailed description of each function is provided in the Supporting information and package documentation. GEE, Google Earth Engine.

Step	Function	Brief Description
Data extraction	*lsat_get_pixel_centers*	(*Optional*) Retrieve point coordinates of all Landsat 8 pixel centers that fall within a polygon.
	lsat_export_ts	Export full Landsat surface reflectance time series for a set of point coordinates using GEE accessed from R.
Data processing	*lsat_format_data*	Prepare data exported from GEE, including parsing satellite names and renaming and scaling bands.
	lsat_clean_data	Filter out measurements based on presence of clouds, water, shadows, oblique view angles, and other criteria.
	lsat_summarize_data	(*Optional*) Summarize data availability at each site, such as total number and years of observations.
	lsat_neighborhood_mean	(*Optional*) For buffered sites, compute band-wise mean surface reflectance across grid cells within the buffer.
	lsat_calc_spectral_index	Calculate a variety of widely used spectral indices, such as the Normalized Difference Vegetation Index (NDVI).
	lsat_calibrate_rf	Cross-calibrate bands or spectral indices from Landsat 5/8 to match Landsat 7 using Random Forest models.
	lsat_calibrate_poly	Cross-calibrate bands or spectral indices from Landsat 5/8 to match Landsat 7 using polynomial regression.
	lsat_fit_phenological_curves	Characterize seasonal land surface phenology at each site by iteratively fitting flexible cubic splines.
	lsat_summarize_growing_seasons	Estimate various phenological metrics from fitted cubic splines, such as annual maximum vegetation greenness.
	lsat_evaluate_phenological_max	(*Optional*) Evaluate estimates of annual maximum vegetation greenness with measurement availability.
Data analysis	*lsat_calc_trend*	Calculate temporal trends using non-parametric Mann–Kendall trend tests and Theil–Sen slope indicators.
	lsat_plot_trend_hist	Plots a histogram of trends across sample sites.

process Landsat data using 'LandsatTS', but then capitalize on tools provided by other R packages (www.r-project.org), such as the new 'phenofit' package that provides state-of-the-art tools for fitting phenological models (Kong et al. 2022). Alternatively, users who are interested in phenological modeling with other data sources (e.g. phenocams, MODIS) could utilize functions from 'LandsatTS'. More broadly, while 'LandsatTS' provides tools focused on generating high-quality vegetation greenness times series, it also enables users to undertake other analyses that rely on cleaned and cross-calibrated Landsat data.

'LandsatTS' includes an integrated suite of tools that were originally developed to assess long-term changes in vegetation greenness within the rapidly warming Arctic tundra and boreal forest biomes (Berner et al. 2020, Berner and Goetz 2022). This software implements a sample-based approach that we found is well suited for assessing vegetation dynamics and evaluating ecological hypotheses in these cold northern biomes, while substantially reducing computational burden compared with wall-to-wall analyses. The sample-based approach is conducive to rigorous propagation of uncertainty using Monte Carlo simulations (Berner et al. 2020, Berner and Goetz 2022), which is important for improving confidence in remote sensing analyses but seldom carried out because of computational constraints (Myers-Smith et al. 2020). Furthermore, the sample-based approach has helped validate and interpret vegetation dynamics inferred from spectral indices by enabling comparisons between satellite and field measurements across widely distributed site networks (Boyd et al. 2019, Berner et al. 2020, Boyd et al. 2021, Walker et al. 2021). These tools have also been used to assess high-latitude vegetation responses to insect outbreaks (Boyd et al. 2019, Boyd et al. 2021), wildfires (Gaglioti et al. 2021), and permafrost degradation (Verdonen et al. 2020), as well as for syntheses focused on high-latitude disturbance regimes (Foster et al. 2022) and Arctic shrubification (Mekonnen et al. 2021). Among other applications, these tools could further be used to complement field-based ecosystems monitoring in protected areas, evaluate ecosystem impacts of extreme weather events (e.g. droughts), and improve local to global mapping efforts by enabling users to develop regression models for cross-sensor calibration. In summary, 'LandsatTS' enables ecologists and other researchers to extract and process Landsat time series that can then be used to analyze vegetation phenology or for other user-defined applications.

Here, we illustrate a typical workflow (Fig. 1) and briefly describe each function (Table 1), as well as provide an example application focused on vegetation dynamics across the Noatak National Preserve, USA, and instructions for package installation. Detailed descriptions of each function are included in the Supporting information and package user manual. Additional examples and information are provided in a vignette that is included as Supporting information and accessible from within R, as well as on the 'LandsatTS' GitHub repository (https://github.com/logan-berner/LandsatTS).

Example application: vegetation greenness trends in the Noatak National Preserve, USA

Here we provide an example analysis of interannual changes in vegetation greenness from 2000 to 2022 within the Noatak National Preserve in northern Alaska, USA (Fig. 2). The Noatak National Preserve is a vast wilderness of mountainous Arctic and alpine tundra that encompasses the largest undisturbed watershed in North America. The preserve is about 2.6 million hectares of roadless lands that were designated in 1980 to maintain ecological integrity, protect habitat and archeological resources, and provide opportunities for scientific research (US National Park Service 2023). Recent ecological research found climate warming substantially increased growth rates of white spruce *Picea glauca* and led to rapid expansion of trees and tall shrubs into tundra over the past half century in parts of the preserve (Suarez et al. 1999, Terskaia et al. 2020, Dial et al. 2022). The impacts of climate change are increasingly evident in the Noatak National Preserve and underscore the importance of sustained and cost-effective ecological monitoring and assessment.

Annual maximum vegetation greenness is related to tundra aboveground biomass and productivity, making it an important ecological metric that can be monitored using satellite remote sensing (Jia et al. 2003, Raynolds et al. 2012, Berner et al. 2018, Bhatt et al. 2021). We therefore demonstrate how multidecadal changes in annual maximum vegetation greenness can be readily assessed across the preserve using Landsat satellite data. In this section, we guide the reader through the analysis code with example output figures and tables that are generated by the 'LandsatTS' functions. Please note that Code Box 1 requires access to GEE for exporting Landsat data; however, Code Boxes 2–4 can be run without access to GEE because they rely on a dataset provided with the package.

Part 1: Export Landsat time series from Google Earth Engine

To start, we create a random sample of points within the Noatak National Preserve and then export Landsat time series for each sample point using GEE (Code Box 1). To facilitate our example, we include the preserve boundary as a simple feature polygon dataset ('noatak.sf') in 'LandsatTS'. Users could alternatively read in their own shapefile using *sf::st_read()* or create a collection of spatial points (e.g. field sites) using *sf::st_sf()* (Pebesma 2018). We load the preserve boundary dataset, create a simple random sample of *n* points

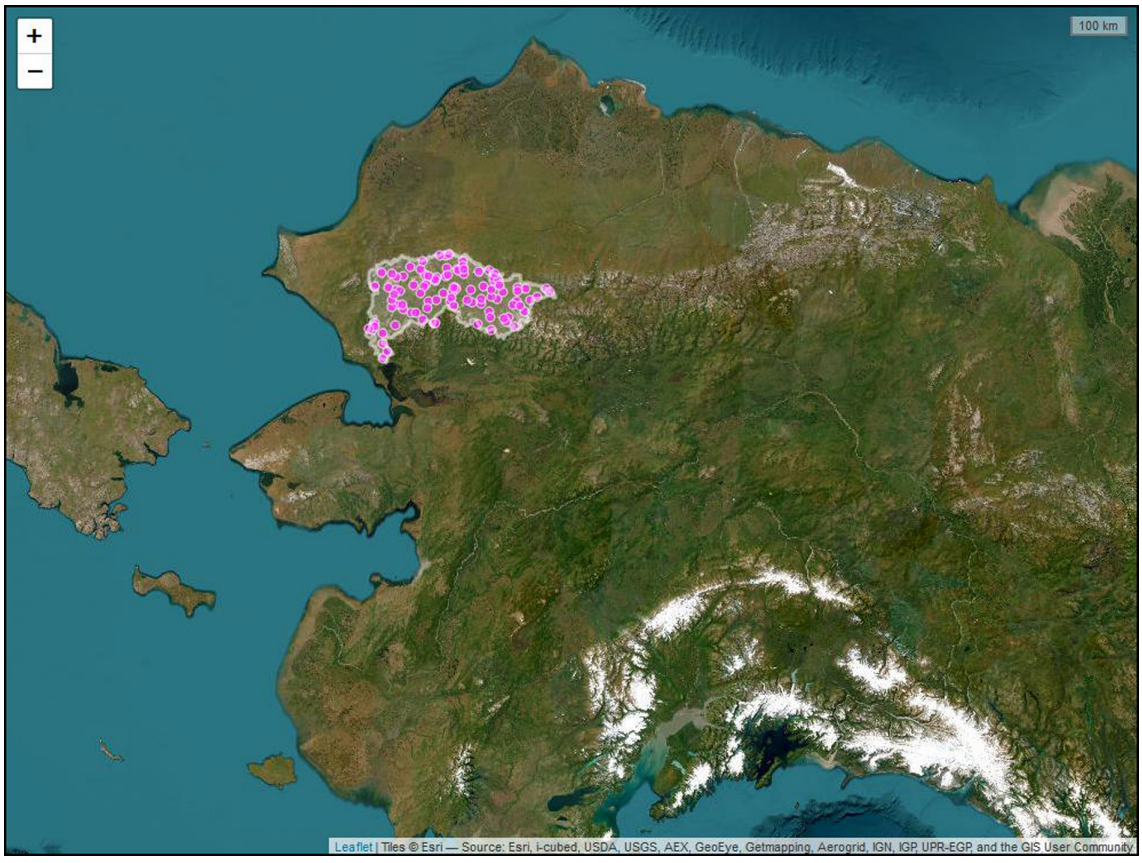

Figure 2. Screenshot of a leaflet interactive map showing the Noatak National Preserve boundary in northern Alaska, USA, and 100 random sample points within the preserve. Landsat time series data were extracted for each of these sample points. Base map from ESRI World Imagery (ESRI 2022).

Code Box 1. Export Landsat time series from Google Earth Engine

```
# Load required R packages
require(LandsatTS)
require(sf)
require(rgee)
require(tidyverse)
require(leaflet)

# Load the Noatak National Preserve simple feature polygon
data(noatak.sf)

# Create n random sample points within the Noatak National Preserve
n.pts <- 3
noatak.pts.sf <- st_sample(x=noatak.sf, size=n.pts) %>% st_sf()

# Add unique identifier to each point
noatak.pts.sf$sample_id <- paste0('S_', 1:n.pts)

# Make interactive map showing Noatak National Preserve and sample points
(Fig. 2)
leaflet() %>%
  addProviderTiles('Esri.WorldImagery') %>%
  addCircleMarkers(data=noatak.pts.sf,
                   color='white',
                   opacity=0.9,
                   fillColor='fuchsia',
                   fillOpacity=0.75,
                   weight=1,
                   radius=5) %>%
  addPolygons(data=noatak.sf,
              color='white',
              weight=3) %>%
  addScaleBar(options=scaleBarOptions(imperial=F))

# Initialize Earth Engine
ee_Initialize()

# Extract a time series of surface reflectance measurements for each Landsat
pixel
task_list <- lsat_export_ts(pixel_coords_sf=noatak.pts.sf,
                            start_date="1985-06-01",
                            end_date="2022-09-30",
                            start_doy=152,
                            end_doy=273,
                            file_prefix='noatak',
                            drive_export_dir='earth_engine')
```

within the boundary using the *sf::st_sample* function, give each sample a unique identifier, and then create an interactive map showing preserve and sample point locations using 'leaflet' (Fig. 2) (Cheng et al. 2022). We then initialize GEE and submit a task to GEE that for each sample point exports all Landsat 5, 7, and 8 measurements made between day of year 152 (beginning of June) and 273 (end of September) from 1985 to 2022. For expediency, this example exports data for three random sample points, which took ~ 11 min and yielded ~ 800 B of data written to a folder called 'earth_engine' on the user's Google Drive. Exporting four decades of summer Landsat data for 100 sample points took ~ 6 h and yielded ~ 28 MB of data, while exporting data for 1000 sample points took ~ 15 h with four tasks running in parallel and yielded ~ 280 MB of data. To facilitate subsequent parts of this example, we include Landsat data for 100 sample points as a dataset ('noatak.dt') in 'LandsatTS'. Data export progress can be monitored using the GEE task manager in the web browser (https://code.earthengine.google.com/tasks) or with the R console using the *ee_monitoring()* function provided by 'rgee'. The CSV file(s) containing the raw exports need to be copied from the user's Google Drive to the local

machine that will carry out the subsequent processing using 'LandsatTS'. The files can be copied manually or using the *rgee::ee_drive_to_local()* function. Once the records are available locally, they need to be cleaned and processed into vegetation index time series as detailed in the next section.

Part 2: Format, clean, and summarize Landsat data in preparation for analysis

We load the Landsat data into R, format and clean the data, and then examine data availability. Here, we provide Landsat data for the 100 sample points as a dataset in 'LandsatTS'; however, the dataset alternatively could be read into R as a data.table using the *fread()* function from the 'data.table' package (Dowle and Srinivasan 2021). Once loaded into R, we format the dataset for analysis using *lsat_format_data()*, which formats column names and scales the band values, among other necessary formatting. We then clean the dataset using *lsat_clean_data()* to filter out clouds, snow, and water, as well as radiometric and geometric errors. For these field sites, *lsat_clean_data()* removed 78 625 of 99 600 observations (78.94%), including one sample point located in water. We then check the availability of clear-sky Landsat observations for the remaining 99 sample points using *lsat_summarize_data*(). On average (± 1 SD), each sample point had 212 ± 48 clear-sky observations made between 1985 and 2022. The annual number of observations is typically small before the year 2000, as highlighted by the figure generated by the function (Fig. 3).

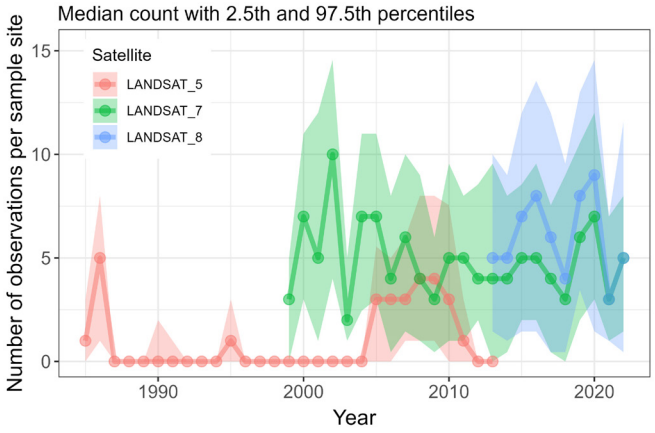

Figure 3. Annual availability of quality screened summer Landsat observations summarized across sample points in the Noatak National Preserve as returned by the function *lsat_summarize_data()*. Summaries are based on observations acquired between day of year 152 (beginning of June) and 273 (end of September). Note the limited availability of observations before the year 2000. Lines with points denote median counts while shaded bands encompass the 2.5th to 97.5th percentiles of counts among sample points.

Part 3: Generate cross-calibrated time series of annual maximum vegetation greenness

To generate time series of annual maximum vegetation greenness for each sample point, we 1) compute NDVI, 2) cross-calibrate NDVI among Landsat sensors, and then 3) estimate annual maximum NDVI (NDVImax) using phenological modeling. First, we calculate NDVI using *lsat_calc_spectral_index()*, which supports calculating a variety of commonly used spectral indices. There are systematic differences in NDVI among Landsat sensors, so next we calibrate NDVI from Landsat 5 TM and Landsat 8 OLI to match Landsat 7 ETM+, which has measurements that temporally overlap with the other two sensors. We cross-calibrate NDVI among sensors using *lsat_calibrate_poly()* to fit and apply polynomial regression models. As the number of field sites

Code Box 2. Format, clean, and summarize Landsat data in preparation for analysis

```
# Load required R packages
require(LandsatTS)
require(data.table)
require(tidyverse)
require(sf)
require(leaflet)
require(mapview)

# Load Landsat data for Noatak sites, or read in file using data.table::fread().
data(noatak.dt)

# Format the exported data
noatak.dt <- lsat_format_data(noatak.dt)

# Clean the data by filtering out clouds, snow, water, etc.
noatak.dt <- lsat_clean_data(noatak.dt)

# Summarize the availability of Landsat data for each pixel (Fig. 3)
lsat_summarize_data(noatak.dt)

# Continue to Code Box 3...
```

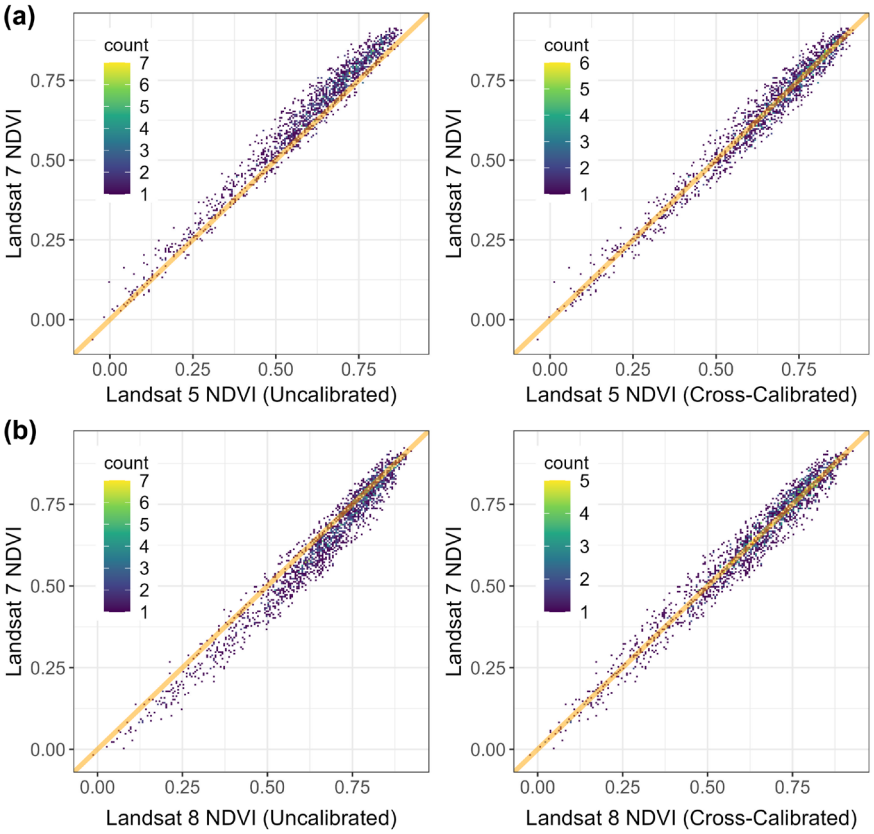

Figure 4. Relationships between Landsat 7 Normalized Difference Vegetation Index (NDVI) and both (a) Landsat 5 NDVI and (b) Landsat 8 NDVI using (left panels) original data and (right panels) data that were calibrated using polynomial regression models. Each point is a sample location from the Arctic–Boreal domain with temporally overlapping measurements from pairs of Landsat sensors. Orange diagonal lines depict 1:1 relationships. Model performance metrics are provided in Table 2. Cross-calibration substantially reduces biases between sensors.

in this dataset is rather small, we use a pre-processed dataset of Landsat observations that were randomly sampled from across northern high-latitudes ecosystems and are included for this purpose with 'LandsatTS'. The function generates and returns a series of graphs (Fig. 4) and tabular data (Table 2) that help with evaluating model performance and can optionally be written to a user-specified directory. As desired, calibration visually (Fig. 4) and statistically (Table 2) reduced the bias between Landsat 7 NDVI and Landsat 5 and 8 NDVI.

As a step towards estimating annual $NDVI_{max}$, we fit phenological models to the calibrated NDVI time series using *lsat_fit_phenological_curves()*. The function automatically returns a figure with Landsat observations and fitted phenological curves for nine random sample locations in the dataset (Fig. 5). Each phenological curve characterizes the seasonal progression of NDVI using observations pooled over a multi-year period (here a 7-year moving window) and should be smooth and hump-shaped. Beware of phenological curves with long straight lines that could suggest inadequate seasonal distribution of data used when fitting the curves. Phenological models were not fit for three sites that were minimally vegetated (NDVI < 0.15) because it is challenging to extract a meaningful vegetation phenology signal under these conditions. After fitting phenological models for 94 field sites, we then generated growing season summary statistics, including estimates of $NDVI_{max}$, using *lsat_summarize_growing_seasons()*. The *lsat_evaluate_phenological_max()* can be used to output a figure that allows for visually assessing the performance of modeled $NDVI_{max}$ (Fig. 6). In the case of the Noatak example dataset, modeled estimates of $NDVI_{max}$ tend to be biased slightly low (~ 1%) when only

Table 2. Summary of original biases, performance of polynomial regression models for cross-sensor calibration, and post-calibration biases in Normalized Difference Vegetation Index (NDVI) between Landsat 7 ETM+ and either Landsat 5 TM or Landsat 8 OLI. Each model was trained using 75% of available data selected at random and then cross-validated using the remaining 25% of data. RMSE, root mean squared error.

	Number of sites		Original data			Cross-validated error metrics			
Satellite sensor	Train	Eval.	RMSE	Median bias	Median % bias	r^2	RMSE	Median bias	Median % bias
Landsat 5 TM	5237	1746	0.052	−0.04	−6.1	0.974	0.032	< 0.01	< 0.1
Landsat 8 OLI	5927	1976	0.050	0.03	4.9	0.965	0.035	< 0.01	< 0.1

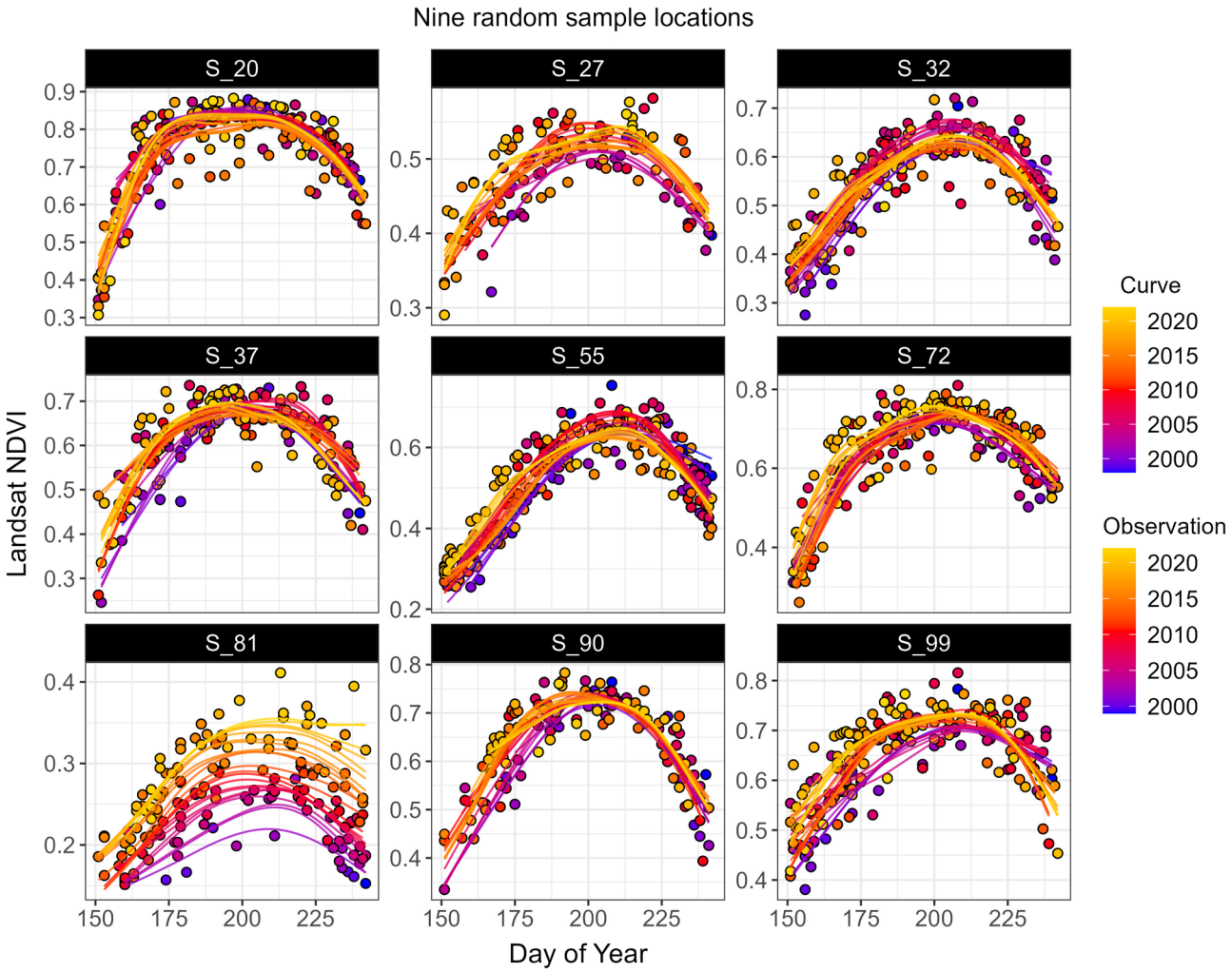

Figure 5. Seasonal progression of Landsat Normalized Difference Vegetation Index (NDVI) and phenological curves for nine random sample points in the Noatak National Preserve. Each dot is an observation that is colored by the year of acquisition ranging between 1985 and 2022. Each line represents a phenological curve that was fit to observations pooled over a 7-year window centered on the focal year as indicated by the color of the line. Color coding helps illustrate how individual curves are fit to observations. These figures can visually highlight long-term changes in phenology and can provide a quick visual assessment of how well curves are being fit to observations, especially when the function is run using the parameter test.run = TRUE.

one or two observations are available from a growing season (Fig. 6), yet there were rarely such few observations during the period from 2000 to 2022 (Fig. 3). The final step following the cross-calibration and phenological modeling is the time series analysis.

Part 4: Analyze vegetation greenness time series

Finally, we evaluate the interannual trend in $NDVI_{max}$ from 2000 to 2022 for each sample point. We calculate temporal trends using the *lsat_calc_trend()* function that implements and summarizes non-parametric trend assessments (Table 3). Note how we use the 'yrs' argument to restrict the time series analysis to the years between 2000 and 2022 to avoid using the low number of observations in the record prior to the turn of the millennium. We then create a histogram of recent $NDVI_{max}$ trends using *lsat_plot_trend_hist()* (Fig. 7) and also create an interactive map showing the trend at each sample point (Fig. 8). These figures indicate extensive greening across the study area in recent decades.

Results and interpretation of the example analysis

Our analysis showed annual maximum vegetation greenness (i.e. $NDVI_{max}$) increased 5.5 ± 10.8% (mean ± 1 SD) from 2000 to 2022 across sample points in the Noatak National Preserve (Fig. 7). During these years, vegetation greenness increased by at least 10% at 20% of sample points. Vegetation greenness systematically ($\alpha = 0.10$) increased at 32% of sample points, decreased at 1% of sample points, and exhibited no systematic change at the remaining 67% of sample points. Greening was especially prevalent in western

Code Box 3. Cross-calibration and phenological modeling

```
# ... continuing from Code Box 2

# Compute the Normalized Difference Vegetation Index (NDVI)
noatak.dt <- lsat_calc_spectral_index(noatak.dt, si='ndvi')

# Cross-calibrate NDVI among sensors using polynomial regression (Fig. 4, Table 2)
noatak.dt <- lsat_calibrate_poly(noatak.dt,
                            band.or.si='ndvi',
                            train.with.highlat.data=T,
                            overwrite.col=T)

# Fit phenological models (cubic splines) to each time series (Fig. 5)
noatak.pheno.dt <- lsat_fit_phenological_curves(noatak.dt, si='ndvi')

# Summarize growing season characteristics
noatak.gs.dt <- lsat_summarize_growing_seasons(noatak.pheno.dt, si='ndvi')

# Evaluate estimates of annual maximum NDVI (Fig. 6)
noatak.gs.eval.dt <- lsat_evaluate_phenological_max(noatak.pheno.dt, si='ndvi')

# Continue to Code Box 4...
```

Code Box 4. Analyze and visualize vegetation greenness time series

```
# ... continuing from Code Box 3

# Compute temporal trend in annual NDVImax for each sample point (Table 3)
noatak.trend.dt <- lsat_calc_trend(noatak.gs.dt, si='ndvi.max', yrs=2000:2022)

# Plot histogram of trends across sample points (Fig. 7)
lsat_plot_trend_hist(noatak.trend.dt, xlim=c(-21,21))

# Create interactive map showing NDVI trends (Fig. 8)
colors.dt <- data.table(trend.cat=c("greening","no_trend","browning"),
 trend.color=c("springgreen","white","orange"))

noatak.trend.dt <- noatak.trend.dt[colors.dt, on='trend.cat']

noatak.trend.sf <- st_as_sf(noatak.trend.dt,
                            coords=c("longitude", "latitude"),
                            crs=4326)

leaflet() %>%
  addProviderTiles('Esri.WorldImagery') %>%
  addPolylines(data=noatak.sf, color='white', weight=3) %>%
  addCircleMarkers(data=noatak.trend.sf,
                   color='white',
                   weight=1,
                   opacity=0.9,
                   fillColor=~trend.color,
                   fillOpacity=0.5,
                   radius=~sqrt(abs(total.change.pcnt))*3) %>%
  setView(-160, 68, zoom=7) %>%
  addLegend('bottomright',
            colors=colors.dt$trend.color,
            labels=colors.dt$trend.cat,
            title='NDVImax trend',
            opacity=1)

# End of code examples
```

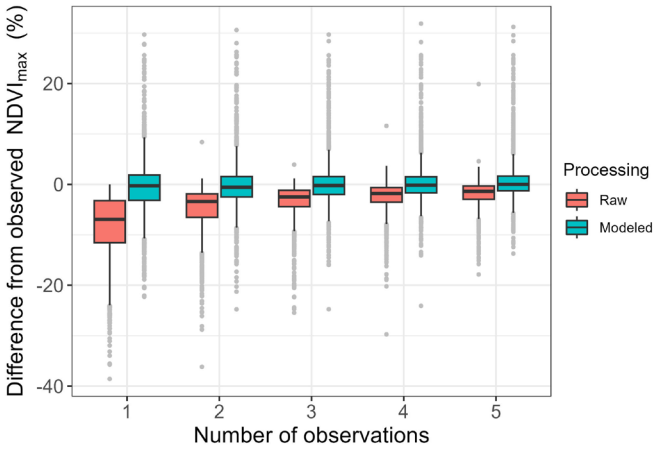

Figure 6. Raw estimates of annual maximum Normalized Difference Vegetation Index (NDVI) ($NDVI_{max}$) are biased low when only a few Landsat observations are available from a given growing season, whereas phenologically modeled estimates of $NDVI_{max}$ are minimally impacted by the availability of observations. The figure summarizes how raw and modeled estimates of $NDVI_{max}$ differ from observed $NDVI_{max}$ based on number of observations, as determined using *lsat_evaluate_phenological_max()*.

parts of the preserve, as well as along in the northern foothills of the Brooks Range (Fig. 8).

These remotely sensed changes suggest tundra productivity and biomass increased in recent decades across large parts of the Noatak National Preserve. These changes are consistent with observed warming-induced expansion of trees and tall shrubs in the preserve (Tape et al. 2006, Terskaia et al. 2020, Dial et al. 2022), as well as with rising summer temperatures increasing the productivity of existing vegetation in this cold tundra environment (Suarez et al. 1999, Berner et al. 2020, Dial et al. 2022). This preserve is also one of the most fire-prone regions in the Arctic and observed greening trends could partially be related to historical fires causing near-surface permafrost thaw, nutrient release, and subsequent shrub proliferation (Gaglioti et al. 2021). Greening in the preserve generally mirrors changes that have been observed more broadly across the Arctic tundra biome, though greening was slightly more prevalent in the preserve than in the broader Arctic (32% versus 27% of sample points, respectively) (Berner et al. 2020, Mekonnen et al. 2021).

This example analysis was based on Landsat data from 100 random sample points, yet nearly identical results were obtained when the analysis was performed using 1000 sample points. Further insight into recent ecological changes could be garnered using a higher sample density with samples stratified by land cover type, ecological land unit, management unit, or other factors (Gaglioti et al. 2021, Berner and Goetz 2022). Nevertheless, Landsat data from even a relatively small random sample (n = 100) enabled robust inference about recent ecological changes that occurred over the past two decades within one of the most remote protected areas in the USA.

Package installation

The R package 'LandsatTS' is publicly available through a GitHub code repository. Users will need to have installed the R software environment on their computer. The 'LandsatTS' package is operating system agnostic and can be installed from within R using the *install_github()* function from the 'devtools' package:

```
devtools::install_github("logan-berner/LandsatTS")
```

If the user would like to access the vignette from within R, then include the argument *build_vignettes = TRUE* when installing the package. Installation will compile the package from source code on the user's computer, as well as acquire and configure external package dependencies (Table 4). However, to use the data extraction and preparation functions, users will need an account on GEE, and to have installed and configured the 'rgee' package to access GEE from R. Please see the GEE (https://earthengine.google.com/) and 'rgee'

Table 3. Abridged summary of annual maximum Normalized Difference Vegetation Index ($NDVI_{max}$) trends from 2000 to 2022 for each sample point (Sample ID) as generated using the function *lsat_calc_trend()*. Trends were assessed for each sample point by removing temporal autocorrelation and then applying a Mann–Kendall trend test (Tau statistic and P-value provided). Slopes were calculated using the Theil–Sen slope estimators.

Sample ID	Latitude	Longitude	N	Slope	Intercept	Tau	P-value	Total change	Total change (%)
S_1	67.70765	−157.404	22	0.00109	0.5918	0.181	0.2639	0.025	4.2
S_10	68.23443	−158.416	23	0.00127	0.6144	0.091	0.5728	0.029	4.7
S_11	67.8104	−157.097	21	0.0017	0.6366	0.105	0.5376	0.039	6.1
S_12	67.81419	−160.017	23	0.00155	0.6943	0.108	0.4986	0.036	5.2
S_13	68.12915	−161.226	23	0.00209	0.5268	0.541	< 0.001	0.048	9.1
S_14	68.26632	−157.32	23	0.00067	0.2369	0.403	0.0095	0.015	6.3
S_15	67.87087	−156.911	22	0.00073	0.6307	0.01	0.9759	0.017	2.7
S_16	68.18229	−156.824	23	0.00048	0.6445	0.065	0.693	0.011	1.7
S_17	67.64494	−158.002	23	0.00314	0.6726	0.541	< 0.001	0.072	10.7
S_18	67.94227	−161.809	23	−0.00086	0.7419	−0.152	0.3377	−0.020	−2.7
S_19	67.76848	−162.447	23	0.00623	0.5918	0.784	< 0.001	0.025	4.2

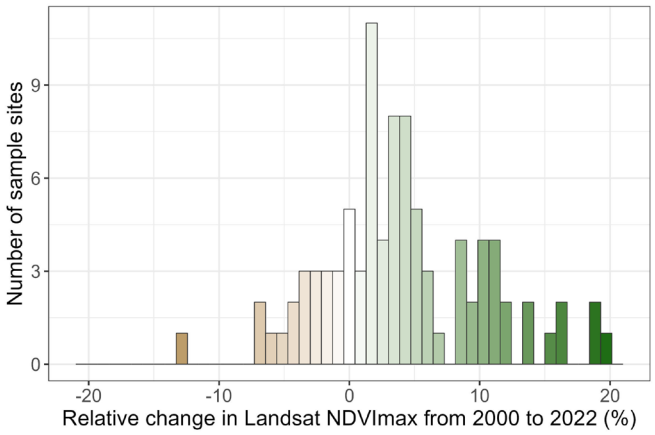

Figure 7. Histogram of relative change in Landsat Normalized Difference Vegetation Index (NDVI) $NDVI_{max}$ from 2000 to 2022 among sample points across the Noatak National Preserve. Relative changes in percent are calculated based on the Theil–Sen slope and intercept estimates (Table 3).

(https://r-spatial.github.io/rgee/) websites for details on signing up for an account and configuring 'rgee', respectively.

Conclusions

The 'LandsatTS' package for R facilitates extracting and processing Landsat surface reflectance time series, as well as generating and analyzing metrics of vegetation greenness and other spectral indices. We demonstrated the functionality of this software by analyzing changes in annual maximum vegetation greenness from 2000 to 2022 across the Noatak National Preserve in northern Alaska, USA. However, we would like to highlight that these tools are also well suited for sample-based analyses of vegetation dynamics across geographic regions ranging from individual field sites to entire terrestrial biomes (Berner et al. 2020, Berner and Goetz 2022). To date, 'LandsatTS' has been used for ecological studies focused on the Arctic tundra and boreal forest biomes, but many of the functions could be used for studies focused on lower latitude ecosystems, especially ecosystems without a multi-modal growing season. Overall, this software provides a suite of functions to enable broader use of Landsat satellite

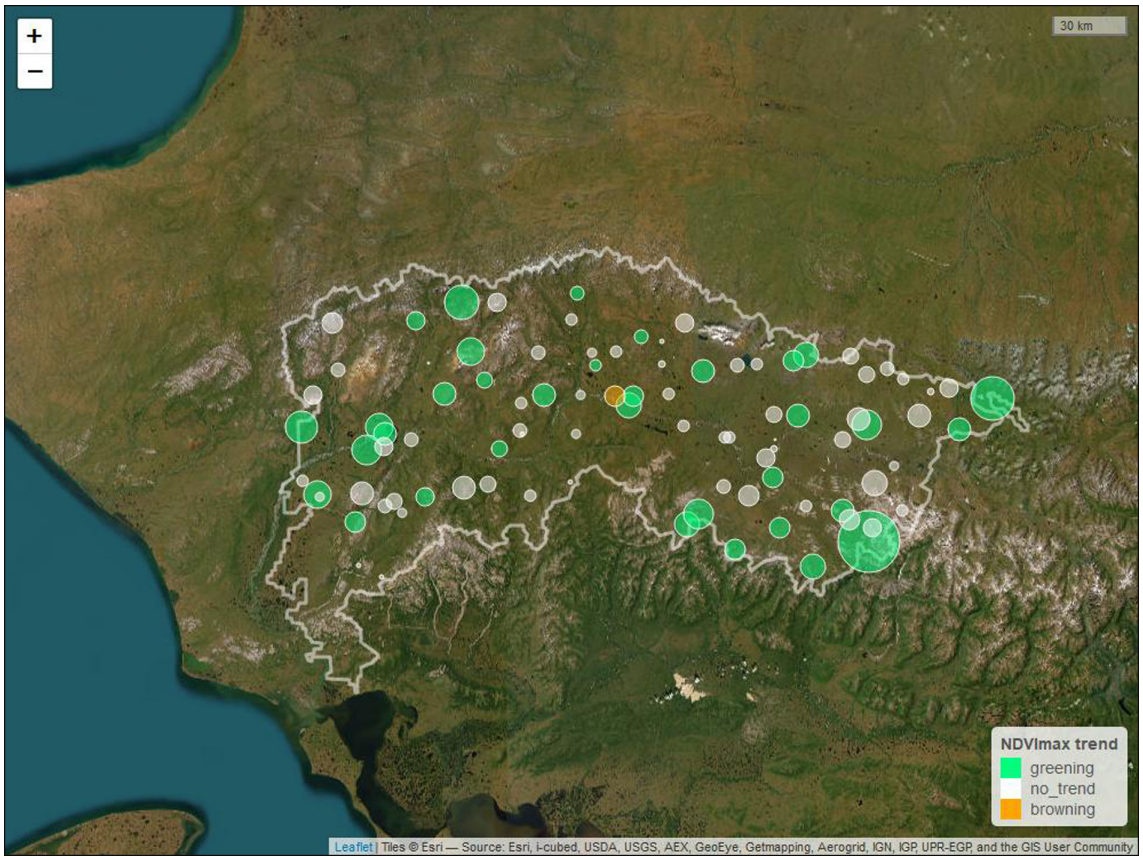

Figure 8. Screenshot of a leaflet interactive map showing the trends in Normalized Difference Vegetation Index (NDVI) NDVImax from 2000 to 2022 for sample points in the Noatak National Preserve located in northern Alaska, USA. The symbol for each sample point is colored based on a combination of NDVImax trend direction and significance ($\alpha = 0.10$), and then sized based on the magnitude of relative change. For leaflet code simplicity, symbol size varies even for sample points without a significantly significant trend. Base map from ESRI World Imagery (ESRI 2022).

Table 4. Package dependencies required by 'LandsatTS', including the package version tested.

Package name	Version	Citation
'crayon'	1.4.2	Csárdi (2021)
'broom'	1.0.4	Robinson et al. (2023)
'data.table'	1.14.2	Dowle and Srinivasan (2021)
'dplyr'	1.0.7	Wickham et al. (2021)
'ggplot2'	3.3.5	Wickham (2016)
'ggpubr'	0.4.0	Kassambara (2020)
'magrittr'	2.0.1	Bache and Wickham (2020)
'mapview'	2.10.0	Appelhans et al. (2021)
'purrr'	0.3.4	Henry and Wickham (2020)
'R.utils'	2.11.0	Bengtsson (2021)
'ranger'	0.13.1	Wright and Ziegler (2017)
'rgee'	1.1.5	Aybar et al. (2020)
'sf'	1.0-4	Pebesma (2018)
'stats'	4.1.1	www.r-project.org
'stringr'	1.4.0	Wickham (2019)
'tidyr'	1.1.4	Wickham (2021)
'zoo'	1.8.9	Zeileis and Grothendieck (2005)
'zyp'	0.10-1.1	Bronaugh and Werner (2019)

data for assessing and monitoring Earth's land surface over the past four decades in a sample-based framework suitable for local to global geographic extents.

To cite 'LandsatTS' or acknowledge its use, cite this Software note as follows, substituting the version of the application that you used for 'ver. 1.0':

Berner, L. T., Assmann, J. J., Normand, S. and Goetz, S. J. 2023. 'LandsatTS': an R package to facilitate retrieval, cleaning, cross-calibration, and phenological modeling of Landsat time series data. – Ecography 2023: e06768 (ver. 1.0).

Acknowledgements – Landsat 5 (doi.org/10.5066/P9IAXOVV), Landsat 7 (doi.org/10.5066/P9C7I13B), and Landsat 8 (doi.org/10.5066/P9OGBGM6) surface reflectance data courtesy of the U.S. Geological Survey. We thank two anonymous reviewers and the subject editor for their valuable feedback.

Funding – We acknowledge support from the National Aeronautics and Space Administration (NASA) Arctic Boreal Vulnerability Experiment (ABoVE) under grant no. 80NSSC19M0112 to S. J. G. and the NASA New Investigator Program (NIP) under grant no. 80NSSC21K1364 to L. T. B. This study was also supported by the National Science Foundation Navigating the New Arctic Big Idea under grant no. 2127273 to L. T. B. and S. J. G. The contributions from J. J. A. and S. N. to this study were funded by the Independent Research Fund of Denmark (grant no. 7027-00133B) and the EU Horizon 2020 CHARTER project (grant agreement no.: 869471).

Author contributions

Logan T. Berner: Conceptualization (lead); Data curation (equal); Formal analysis (lead); Funding acquisition (equal); Investigation (lead); Methodology (lead); Software (lead); Visualization (lead); Writing – original draft (lead); Writing – review and editing (lead). **Jakob J. Assmann**: Conceptualization (equal); Data curation (equal); Formal analysis (equal); Investigation (equal); Methodology (lead); Software (lead); Visualization (equal); Writing – original draft (equal); Writing – review and editing (equal). **Signe Normand**: Funding acquisition (equal); Project administration (equal); Resources (supporting); Supervision (equal); Writing – original draft (supporting); Writing – review and editing (supporting). **Scott J. Goetz**: Conceptualization (supporting); Funding acquisition (lead); Methodology (supporting); Project administration (equal); Resources (equal); Supervision (lead); Writing – original draft (supporting); Writing – review and editing (supporting).

Transparent peer review

The peer review history for this article is available at https://publons.com/publon/10.1111/ecog.06768.

Data availability statement

No new data were generated for this article.

Supporting information

The Supporting information associated with this article is available with the online version.

References

Appelhans, T., Detsch, F., Reudenbach, C. and Woellauer, S. 2021. mapview: interactive viewing of spatial data in R, R package ver. 2.10.0. – https://CRAN.R-project.org/package=mapview.

Aybar, C., Wu, Q., Bautista, L., Yali, R. and Barja, A. 2020. rgee: an R package for interacting with Google Earth Engine. – J. Open Source Softw. 5: 2272.

Bache, S. M. and Wickham, H. 2020. magrittr: a forward-pipe operator for R, R package ver. 2.0.1. – https://CRAN.R-project.org/package=magrittr.

Bengtsson, H. 2021. R.utils: various programming utilities. R package ver. 2.11.0. – https://CRAN.R-project.org/package=R.utils.

Berner, L. T. and Goetz, S. J. 2022. Satellite observations document trends consistent with a boreal forest biome shift. – Glob. Change Biol. 28: 3275–3292.

Berner, L. T., Jantz, P., Tape, K. D. and Goetz, S. J. 2018. Tundra plant aboveground biomass and shrub dominance mapped across the North Slope of Alaska. – Environ. Res. Lett. 13: 035002.

Berner, L. T., Massey, R., Jantz, P., Forbes, B. C., Macias-Fauria, M., Myers-Smith, I. H., Kumpula, T., Gauthier, G., Andreu-Hayles, L., Gaglioti, B. V., Burns, P. J., Zetterberg, P., D'Arrigo, R. and Goetz, S. J. 2020. Summer warming explains widespread but not uniform greening in the Arctic tundra biome. – Nat. Commun. 11: 4621.

Bhatt, U. S., Walker, D. A., Raynolds, M. K., Walsh, J. E., Bieniek, P. A., Cai, L., Comiso, J. C., Epstein, H. E., Frost, G. V., Gersten, R., Hendricks, A. S., Pinzon, J. E., Stock, L. and Tucker, C. J. 2021. Climate drivers of Arctic tundra variability and change using an indicators framework. – Environ. Res. Lett. 16: 055019.

Boyd, M. A., Berner, L. T., Doak, P., Goetz, S. J., Rogers, B. M., Wagner, D., Walker, X. J. and Mack, M. C. 2019. Impacts of

climate and insect herbivory on productivity and physiology of trembling aspen (*Populus tremuloides*) in Alaskan boreal forests. – Environ. Res. Lett. 14: 085010.
Boyd, M. A., Berner, L. T., Foster, A. C., Goetz, S. J., Rogers, B. M., Walker, X. J. and Mack, M. C. 2021. Historic declines in growth portend trembling aspen death during a contemporary leaf miner outbreak in Alaska. – Ecosphere 12: e03569.
Bronaugh, D. and Werner, A. 2019. zyp: Zhang + Yue-Pilon trends package, R package ver. 0.10-1.1. – https://CRAN.R-project.org/package=zyp.
Cheng, J., Karambelkar, B. and Xie, Y. 2022. leaflet: create interactive web maps with the JavaScript 'Leaflet' library, R package ver. 2.1.1. – https://CRAN.R-project.org/package=leaflet.
Csárdi, G. 2021. crayon: colored terminal Output, R package ver. 1.4.2. – https://CRAN.R-project.org/package=crayon.
Dial, R. J., Maher, C. T., Hewitt, R. E. and Sullivan, P. F. 2022. Sufficient conditions for rapid range expansion of a boreal conifer. – Nature 608: 546–551.
dos Santos, A. 2017. landsat8: landsat 8 imagery rescaled to reflectance, radiance and/or temperature, R package ver. 0.1-10. – https://CRAN.R-project.org/package=landsat8.
Dowle, M. and Srinivasan, A. 2021. data.table: extension of 'data.frame', R package ver. 1.14.2. – https://CRAN.R-project.org/package=data.table.
ESRI 2022. ESRI World Imagery. – https://doc.arcgis.com/en/data-appliance/2022/maps/world-imagery.htm.
Foster, A. C. et al. 2022. Disturbances in North American boreal forest and Arctic tundra: impacts, interactions, and responses. – Environ. Res. Lett. 17: 113001.
Gaglioti, B. V., Berner, L. T., Jones, B. M., Orndahl, K. M., Williams, A. P., Andreu-Hayles, L., D'Arrigo, R. D., Goetz, S. J. and Mann, D. H. 2021. Tussocks enduring or shrubs greening: alternate responses to changing fire regimes in the Noatak River Valley, Alaska. – J. Geophys. Res. Biogeosci. 126: e2020JG006009.
Gorelick, N., Hancher, M., Dixon, M., Ilyushchenko, S., Thau, D. and Moore, R. 2017. Google Earth Engine: planetary-scale geospatial analysis for everyone. – Remote Sens. Environ. 202: 18–27.
Goslee, S. 2011. Analyzing remote sensing data in R: the Landsat package. – J. Stat. Softw. 43: 1–25.
Hansen, M. C., Potapov, P. V., Moore, R., Hancher, M., Turubanova, S. A., Tyukavina, A., Thau, D., Stehman, S. V., Goetz, S. J., Loveland, T. R., Kommareddy, A., Egorov, A., Chini, L., Justice, C. O. and Townshend, J. R. G. 2013. High-resolution global maps of 21st-century forest cover change. – Science 342: 850–853.
Helman, D. 2018. Land surface phenology: what do we really 'see' from space? – Sci. Total Environ. 618: 665–673.
Henry, L. and Wickham, H. 2020. purrr: functional programming tools, R package ver. 0.3.4. – https://CRAN.R-project.org/package=purrr.
Jia, G. J., Epstein, H. E. and Walker, D. A. 2003. Greening of arctic Alaska, 1981–2001. – Geophys. Res. Lett. 30: 2067.
Ju, J. and Masek, J. G. 2016. The vegetation greenness trend in Canada and US Alaska from 1984–2012 Landsat data. – Remote Sens. Environ. 176: 1–16.
Kassambara, A. 2020. ggpubr: 'ggplot2' based publication ready plots, R package ver. 0.4.0. – https://CRAN.R-project.org/package=ggpubr.
Kong, D., McVicar, T. R., Xiao, M., Zhang, Y., Peña-Arancibia, J. L., Filippa, G., Xie, Y. and Gu, X. 2022. phenofit: an R package for extracting vegetation phenology from time series remote sensing. – Methods Ecol. Evol. 13: 1508–1527.
Lai, J., Lortie, C. J., Muenchen, R. A., Yang, J. and Ma, K. 2019. Evaluating the popularity of R in ecology. – Ecosphere 10: e02567.
Mekonnen, Z. A., Riley, W. J., Berner, L. T., Bouskill, N. J., Torn, M. S., Iwahana, G., Breen, A. L., Myers-Smith, I. H., Criado, M. G., Liu, Y., Euskirchen, E. S., Goetz, S. J., Mack, M. C. and Grant, R. F. 2021. Arctic tundra shrubification: a review of mechanisms and impacts on ecosystem carbon balance. – Environ. Res. Lett. 16: 053001.
Myers-Smith, I. H. et al. 2020. Complexity revealed in the greening of the Arctic. – Nat. Clim. Change 10: 106–117.
National Academies of Sciences 2018. Thriving on our changing planet: a decadal strategy for earth observation from space. – The National Academies Press.
Pebesma, E. J. 2018. Simple features for R: standardized support for spatial vector data. – R J. 10: 439–446.
Pekel, J. F., Cottam, A., Gorelick, N. and Belward, A. S. 2016. High-resolution mapping of global surface water and its long-term changes. – Nature 540: 418–422.
Potapov, P., Hansen, M. C., Pickens, A., Hernandez-Serna, A., Tyukavina, A., Turubanova, S., Zalles, V., Li, X., Khan, A., Stolle, F., Harris, N., Song, X.-P., Baggett, A., Kommareddy, I. and Kommareddy, A. 2022. The global 2000–2020 land cover and land use change dataset derived from the Landsat archive: first results. – Front. Remote Sens. 3: 856903.
Powell, S. L., Cohen, W. B., Healey, S. P., Kennedy, R. E., Moisen, G. G., Pierce, K. B. and Ohmann, J. L. 2010. Quantification of live aboveground forest biomass dynamics with Landsat time-series and field inventory data: a comparison of empirical modeling approaches. – Remote Sens. Environ. 114: 1053–1068.
Raynolds, M. K., Walker, D. A., Epstein, H. E., Pinzon, J. E. and Tucker, C. J. 2012. A new estimate of tundra-biome phytomass from trans-Arctic field data and AVHRR NDVI. – Remote Sens. Lett. 3: 403–411.
Robinson, D., Hayes, A. and Couch, S. 2023. broom: convert statistical objects into tidy tibbles, R package ver. 1.0.4. – https://CRAN.R-project.org/package=broom.
Roy, D. P., Kovalskyy, V., Zhang, H. K., Vermote, E. F., Yan, L., Kumar, S. S. and Egorov, A. 2016. Characterization of Landsat-7 to Landsat-8 reflective wavelength and normalized difference vegetation index continuity. – Remote Sens. Environ. 185: 57–70.
Sexton, J. O., Song, X.-P., Feng, M., Noojipady, P., Anand, A., Huang, C., Kim, D., Collins, K. M., Channan, S., DiMiceli, C. and Townshend, J. R. 2013. Global, 30-m resolution continuous fields of tree cover: Landsat-based rescaling of MODIS vegetation continuous fields with lidar-based estimates of error. – Int. J. Digit. Earth 6: 427–448.
Suarez, F., Binkley, D., Kaye, M. W. and Stottlemyer, R. 1999. Expansion of forest stands into tundra in the Noatak National Preserve, northwest Alaska. – Ecoscience 6: 465–470.
Sulla-Menashe, D., Woodcock, C. E. and Friedl, M. A. 2018. Canadian boreal forest greening and browning trends: an analysis of biogeographic patterns and the relative roles of disturbance versus climate drivers. – Environ. Res. Lett. 13: 014007.
Tape, K., Sturm, M. and Racine, C. 2006. The evidence for shrub expansion in Northern Alaska and the Pan-Arctic. – Glob. Change Biol. 12: 686–702.
Terskaia, A., Dial, R. J. and Sullivan, P. F. 2020. Pathways of tundra encroachment by trees and tall shrubs in the western Brooks Range of Alaska. – Ecography 43: 769–778.

US National Park Service 2023. Noatak National Preserve. – www.nps.gov/noat/index.htm.
Verdonen, M., Berner, L. T., Forbes, B. C. and Kumpula, T. 2020. Periglacial vegetation dynamics in Arctic Russia: decadal analysis of tundra regeneration on landslides with time series satellite imagery. – Environ. Res. Lett. 15: 105020.
Walker, X. J., Alexander, H. D., Berner, L. T., Boyd, M. A., Loranty, M. M., Natali, S. M. and Mack, M. C. 2021. Positive response of tree productivity to warming is reversed by increased tree density at the Arctic tundra-taiga ecotone. – Can. J. Forest Res. 51: 1323–1338.
Wang, J. A. and Friedl, M. A. 2019. The role of land cover change in Arctic-Boreal greening and browning trends. – Environ. Res. Lett. 14: 125007.
Wickham, H. 2016. ggplot2: elegant graphics for data analysis. – Springer-Verlag.
Wickham, H. 2019. stringr: simple, consistent wrappers for common string operations, R package ver. 1.4.0. – https://CRAN.R-project.org/package=stringr.
Wickham, H. 2021. tidyr: tidy Messy Data, R package ver. 1.1.4. – https://CRAN.R-project.org/package=tidyr.
Wickham, H., Francois, R., Lionel, H. and Müller, K. 2021. dplyr: a grammar of data manipulation, R package ver. 1.0.7. – https://CRAN.R-project.org/package=dplyr.
Wright, M. N. and Ziegler, A. 2017. Ranger: a fast implementation of random forests for high dimensional data in C++ and R. – J. Stat. Softw. 77: 1–17.
Wulder, M. A., Skakun, R. S., Kurz, W. A. and White, J. C. 2004. Estimating time since forest harvest using segmented Landsat ETM+ imagery. – Remote Sens. Environ. 93: 179–187.
Wulder, M. A., Masek, J. G., Cohen, W. B., Loveland, T. R. and Woodcock, C. E. 2012. Opening the archive: how free data has enabled the science and monitoring promise of Landsat. – Remote Sens. Environ. 122: 2–10.
Wulder, M. A. et al. 2019. Current status of Landsat program, science, and applications. – Remote Sens. Environ. 225: 127–147.
Zeileis, A. and Grothendieck, G. 2005. zoo: S3 infrastructure for regular and irregular time series. – J. Stat. Softw. 14: 1–27.
Zeng, L., Wardlow, B. D., Xiang, D., Hu, S. and Li, D. 2020. A review of vegetation phenological metrics extraction using time-series, multispectral satellite data. – Remote Sens. Environ. 237: 111511.
Zhu, Z., Wang, S. and Woodcock, C. E. 2015. Improvement and expansion of the Fmask algorithm: cloud, cloud shadow, and snow detection for Landsats 4–7, 8, and Sentinel 2 images. – Remote Sens. Environ. 159: 269–277.